CrossMark

ORIGINAL PAPER

A dynamic dissolution model of rock salt under gravity for different flow rates

Xinrong Liu[1,2] · Xin Yang[1,2] · Junbao Wang[3] · Dongliang Li[1,2] · Peng Li[1,2] ·
Zhongping Yang[1,2]

Abstract The dissolution mechanism of rock salt under the effect of gravity was investigated in the laboratory using a dynamic dissolution test apparatus. Rock salt specimens were subjected to dissolution at different flow rates and the weight of the dissolved salt was measured over time and a comparison between the dissolution weight changes under the effect of gravity of this paper and those of dissolution without considering the gravitational effect was analyzed. After introducing the partial differential equations of a dynamic dissolution which conducted in a non-gravity condition, the influence of different parameters on the dissolution model was discussed to establish the dynamic dissolution model of rock salt under gravitational effect. Then, a numerical solution based on the finite-difference method and parameter inversion was conducted, whose numerical calculation results were in good agreement with the experimental results. The results of this paper can provide a basic theoretical foundation and analytical means that can serve a guide for studies on the dissolution mechanism of rock salt.

Keywords Rock salt · Dissolution model · Gravity · Flow rates · Finite-difference method

✉ Xin Yang
yangxin546@163.com

[1] School of Civil Engineering, Chongqing University, Chongqing 400045, China

[2] Key Laboratory of New Technology for Construction of Cities in Mountain Area, Ministry of Education, Chongqing University, Chongqing 400030, China

[3] College of Civil Engineering, Xi'an University of Architecture and Technology, Xi'an 710055, China

Introduction

Energy in the form of oil or natural gas is an essential factor in a country's economy and affects to both national welfare and people's livelihood. There are three main methods of energy storage: land storage tanks, maritime storage tanks, and underground storage. Of the three methods, underground storage is the safest way of energy storage, known as "the reserve warehouse of highly strategic security." Compared with other rocks, rock salt has many advantages as a medium for energy underground storage in the form of rock salt caverns. At present, research on rock salt is focused mainly on aspects of stability analysis and the mechanical properties of rock salt. Tsang et al. (2005) used laboratory tests and theoretical analysis to investigate cavern excavation damage zone of rock salt. Wawersik (1981) and Cosenza et al. (1999) measured the permeability of rock salt in their study of long-term stability of gas storage. Stormont (1997) measured gas permeability of rock salt in laboratory tests and described the damage that occurred in the rock salt. Hampel and Schulze (2007) analyzed the basic mechanical parameters of a constitutive model of rock salt. Yang et al. (2013) examined the risks of gas storage in a laminar rock salt cave, and Liang et al. (2008) established the coupling theory of the dissolution and seepage effects on mass transmission and the mechanical properties of rock salt.

Many scholars have studied the dissolution characteristics of rock salt in different conditions (Liu et al. 2002; Jiang et al. 2009; Ma et al. 2010; Tang et al. 2012; Zhou et al. 2006; Jessen 1972; Liu et al. 2015), mainly through experimental investigations. In this paper, based on dissolution test data of rock salt, a dynamic dissolution model of rock salt subjected to gravity is established which is solved using the finite-difference method, which can provide basic parameters constructing rock salt cavities.

Springer

Experimental research on the dynamic dissolution properties of rock salt under gravitational effect

Experimental process

The specimens for the experiments were obtained from natural rock salt from the Himalayan Mountains in Pakistan. The bulk rock salt was processed into test specimens 50×100 mm. The specimens were comprised of 99.8 % soluble substance with an average density of 2059 kg/m^3 (Table 1).

A water-passage pinhole of 0.6 cm diameter was drilled at the center of the sample's axial position and processing conducted strictly in line with the experimental regulations. Figure 1 depicts the rock salt samples prepared for hole-boring.

The apparatus for testing the dynamic dissolution was designed specifically for this experiment (Fig. 2). The testing equipment included the following: iron pedestal, beaker chain clip, 703 glue, two large beakers, liquid flowmeter (range 6–60 L/h), tissue, air blower, high precision electronic scales (precision 0.01 g), plastic pipe (outer diameter of 0.6 cm), and a vernier caliper.

The experimental procedure is as follows:

(1) Each drilled specimen is weight using electronic scales, and its length and diameter are measured using the vernier caliper.
(2) Each specimen is coated with a waterproof sealant material (703 silicone glue) and then weighed by electronic scales.
(3) The tap water flow from the faucet is firstly adjusted to 10 L/h.
(4) The sealed specimen is firmly attached to the beaker chain clip, and the water pipe is inserted into the specimen for the rock salt dynamic dissolution test.
(5) After 3 min, the water pipe is pulled out of the specimen and the pipe directed into another large beaker to ensure flow stability. The specimen is removed from the testing device, wiped dry, blow-dried with an air blower, and weighed with the electronic scales.

Fig. 1 Rock salt samples

(6) Step (4) is repeated until dissolved to the boundary of specimen.
(7) Steps (4), (5), and (6) are repeated for water flows of 20 L/h, 30 L/h, and 40 L/h.

Test results

Table 2 Rock salt test specimens—pre-test parameters

Sample no.	Diameter (mm)	Length (mm)	Mass of specimen (g)	Mass of sealed and waterproofed specimen (g)	Density (g·cm^{-3})
B1	52.86	99.7	458.52	465.79	2.1241
B2	51.38	103.42	457.15	463.35	2.1625
B3	52.66	102.56	433.64	439.59	1.9679
B4	52.1	98.82	437.69	444.72	2.1435

Table 3 Test results of dynamic dissolution of rock salt subjected to gravity—specimen weight in (g)

Flow rate Time (min)	10 L/h B1	20 L/h B2	30 L/h B3	40 L/h B4
0	465.79	463.35	439.59	444.72
3	461.18	456.25	428.93	427.73
6	455.42	444.67	413.06	408.95
9	448.13	429.95	393.98	383.35
12	446.57	411.97	376.52	360.15
15	436.22	392.48	353.38	330.96
18	426.5	371.08	326.76	305.35
21	414.58	353.1	306.63	277.67
24	402.57	338.18	288.78	
27	389.32	319.47		
30	374.94	293.45		
33	359.49	266.23		
36		238.08		

Table 1   Components of rock salt specimens (%)

Soluble substance		Insoluble substance
NaCl	K$_2$SO$_3$	Small amount of mud
99.4	0.4	0.2

Fig. 2 Apparatus for testing dynamic dissolution of rock salt under the effect of gravity

Plastic pipe and connector
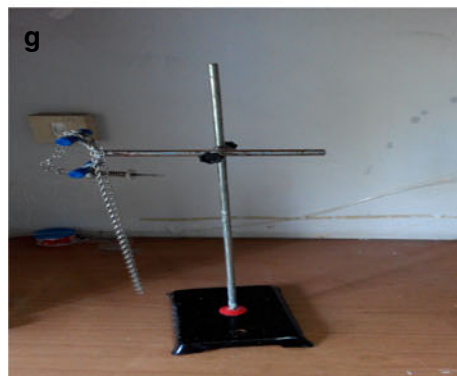
Connector

Devices (a) and (b) connected

Fluid flowmeter

Faucet

Faucet connected to device (c)

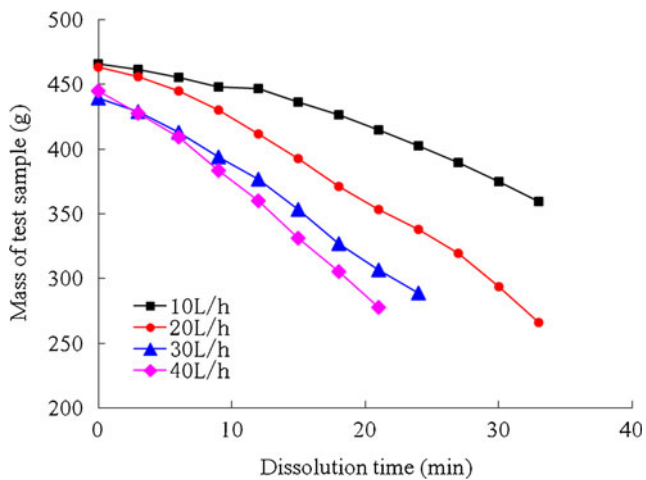Iron pedestal and beaker chain clip

Dissolution test apparatus

Fig. 3 Specimen mass after dissolution under gravitational effect at different flow rates
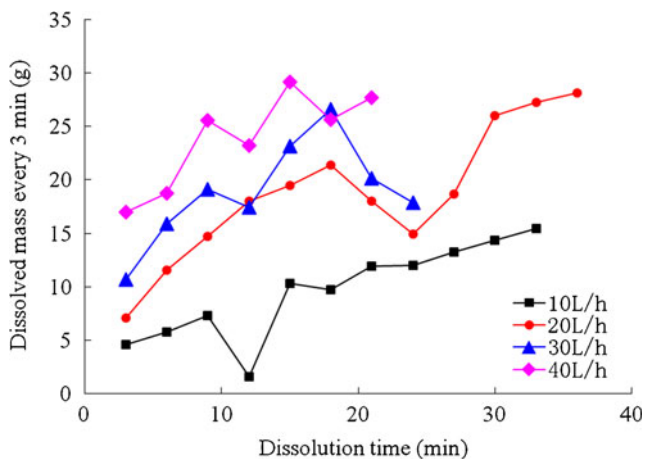

Fig. 4 Specimen dissolved mass measured every 3 min under gravitational effect for different flow rates.

Analysis of test results

The curves of the specimen mass, the dissolved mass with time, and test specimens after dissolution are shown in Figs. 3, 4, and 5, respectively. From Fig. 4, we can see the curve of the dynamic dissolution weight of the rock salt specimen is not smooth, but fluctuates with time. Moreover, as the flow rate Q increased, the dissolution rate of the specimen also increased and the dissolution weight change became more obvious, indicating that the movement of the solution accelerated its convection and diffusion.

Test specimen after dissolution for flow rate of 20 L/h

Test specimen after dissolution for flow rate of 30 L/h
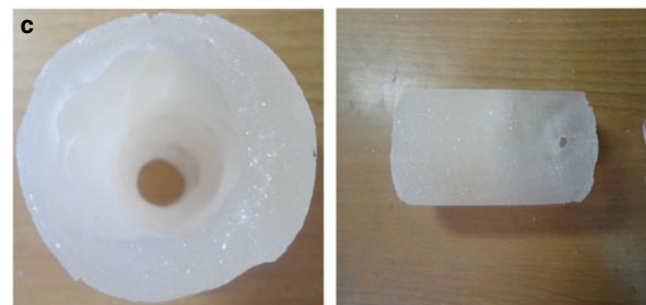
Test specimen after dissolution for flow rate of 40 L/h

Fig. 5 Test specimens after dissolution test

Our results were consistent with those of Liu et al. (2015) for the three flow rates of 20, 30, and 40 L/h, which conducted in a non-gravity condition. The dissolution weight changes under the effect of gravity of this paper were larger than those of Liu et al. (2015) without considering the gravitational effect. Without gravity, the average dissolution rates at water flows of 20, 30, and 40 L/h were 2.8388, 3.7295, and 5.4354 g/min, while under gravitational effect, the average dissolution rates were 5.9733, 6.2838, and 7.9548 g/min, respectively. The average dissolution rates under gravity effect were 2.1041, 1.6848, and 1.4635 times of those without gravity for flow rates of 20, 30, and 40 L/h, respectively, indicating that the gravity effect increased the water flow and accelerated the dissolution of the rock salt. Because the dissolution mechanism of rock salt under gravity effect is the sum of two parts: dissolution without gravitational effect and dissolution generated by the increasing flow velocity under the effect of gravity, as shown in Fig. 6.

Dynamic dissolution model of rock salt subjected to gravity

As shown in the previous section, the dissolution rates under the effect of gravity were greater than without considering the gravitational effect. Increased dissolution rates would raise the concentration level of the water-salt solution. Hence, the solution concentration increased, leading to a faster dissolution.

To establish the dynamic dissolution model of rock salt under gravity, we considered two hypotheses.

(1) The first hypothesis suggests that the effect of gravity increased the flow rate Q.

Liu et al. (2015) present the partial differential equations (Eq. (1)) of a dynamic dissolution model which conducted in a non-gravity condition describing the changes in the dissolved radius R and solution concentration C:

$$\begin{cases} \dfrac{\partial R}{\partial t} = \dfrac{2}{\delta} D \dfrac{M}{\rho_s}(C_s - C_{xt}) \\ \dfrac{\partial C}{\partial x} = \dfrac{2D}{\delta Q}\pi(d + 2R_{xt})(C_s - C_{xt}) \\ R_{xt}|_{t=0} = 0 \\ C_{xt}|_{x=0} = C_0 \end{cases} \quad (1)$$

where, C_0 refers to the initial concentration, C_s represents saturation concentration of the rock salt solution (mol·L^{-1}), C_{xt} refers to the concentration of solution at the section position of x with the time period of t, (mol·L^{-1}), D represents the diffusive coefficient (cm^{-2}·s^{-1}), δ refers to the boundary layer's thickness (cm), ρ_s refers to the density of rock salt (cm^3·s^{-1}), M represents the molar mass of rock salt (g·mol^{-1}), R is the dissolved radius of the rock salt specimen (cm), and d represents the diameter of the pinhole (cm).

Equation (1) indicates that if Q increases under gravitational effect, C would decrease. This is contradictory to our test results. According to Eq. (1), which showed a gradual rise in C along the direction of the flow movement, the dissolved radius R decreases gradually along the direction of the flow movement; this too does not reflect our test results.

Therefore, based on this hypothesis, the dissolution equation is inconsistent with the dynamic dissolution test results of rock salt under gravity, leading us to explore the second hypothesis.

(2) The second hypothesis proposes that the effect of gravity raises the value of parameter D/δ.

It assumes that the parameter D/δ in Eq. (1) was not an invariable constant that increases as the flow rate Q becomes higher. As Q increases under the effect of gravity, C increases as D/δ increases, the dissolved radius R also increases along the direction of the flow movement due to the rise in the value of D/δ. Therefore, this hypothesis could well explain the test results of dynamic dissolution under gravity.

In Liu et al. (2015), the parameter D/δ was fitted for the various flow rates to obtain the values shown in Table 4. The relationship between the flow quantity Q and the parameter D/δ was acquired by linear fitting, where $D/\delta = 0.00005039Q + 0.0005421$, with a correlation coefficient 0.9999. The research result showed that the flow quantity Q was linear with the parameter D/δ.

The linear relationship between Q and D/δ indicates that the parameter D/δ and the flow velocity follow a similar trend. In the dynamic dissolution process of rock salt, we introduce a transformation coefficient α which conformed to the following relation:

$$\frac{D}{\delta} = \alpha V_g \quad (2)$$

where, V_g is the flow velocity (cm·s^{-1}) under the effect of gravity.

The flow velocity under gravity V_g can be simplified as an acceleration process with an initial velocity Q/A and an

Fig. 6 Illustration of dissolution mechanism under gravitational effect
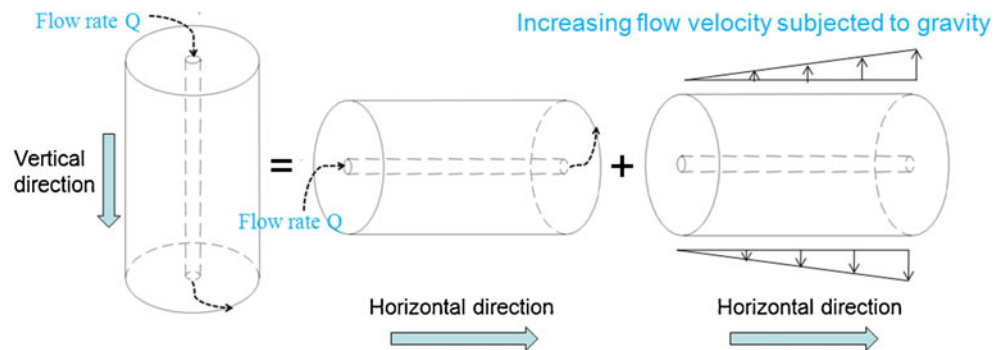
Flow rate Q

Increasing flow velocity subjected to gravity

Vertical direction

Flow rate Q

Horizontal direction

Horizontal direction

Table 4 Parameter D/δ for various flow rates (Liu et al. 2015)

Q L/h	D/δ cm/s
20	0.001554
30	0.002043
40	0.002567
50	0.003059

acceleration of 980 cm · s^{-2} over a distance H (H is the position head). Thus, we obtain the following:

$$V_g = \sqrt{\left(\frac{Q}{A}\right)^2 + 1960H} \quad (3)$$

Substituting Eqs. (2) and (3) into Eq. (1), the dissolution model under gravitational effect can be acquired as follows:

$$
\begin{cases}
\dfrac{\partial R}{\partial t} = \dfrac{M}{\rho_s}\left[2\alpha\left(\sqrt{\left(\dfrac{Q}{A}\right)^2 + 1960H}\right)(C_s - C_{xt})\right] \\[2ex]
\dfrac{\partial C}{\partial x} = \dfrac{\pi}{Q}(d + 2R_{xt})\left[2\alpha\left(\sqrt{\left(\dfrac{Q}{A}\right)^2 + 1960H}\right)(C_s - C_{xt})\right] \\[2ex]
R_{xt}\big|_{t=0} = 0 \\
C_{xt}\big|_{x=0} = C_0
\end{cases}
\quad (4)
$$

Numerical solutions and analysis of the rock salt dynamic dissolution model under gravity

Numerical solution

Because of the interaction between the velocity field and concentration field, Eq. (4) is nonlinear and an analytical solution is difficult to obtain; therefore, to acquire a suitable difference scheme, the partial differential equations (Eq. (4)) were discretized and solved by a finite-difference method.
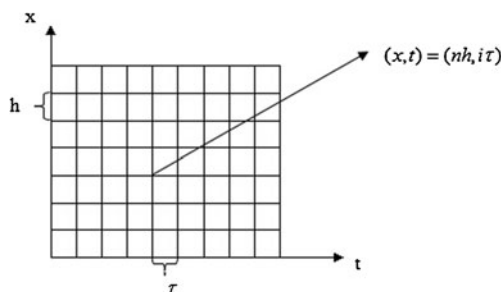

Fig. 7 Finite-difference grid for the dissolution model

The finite-difference model grid is shown in Fig. 7, where the interval in x direction is h and the interval in t direction is τ. And

$$
\begin{cases}
R(x,t) = R(nh, i\tau) = R_i^n \\
C(x,t) = C(nh, i\tau) = C_i^n \\
\dfrac{\partial R(x,t)}{\partial t} = \dfrac{\partial R}{\partial t} \\
\dfrac{\partial C(x,t)}{\partial x} = \dfrac{\partial C}{\partial x}
\end{cases}
\quad (5)
$$

We took the center difference to the area parameter A, and the difference scheme was established based on Eq. (4) as follows:

$$
\begin{cases}
\dfrac{R(nh, (i+1)\tau) - R(nh, i\tau)}{\tau} = \dfrac{M}{\rho_s}\Bigg[2\alpha\Bigg(C_s - \\
\quad C(nh, i\tau)\Bigg)\Bigg(\sqrt{\left(\dfrac{2Q}{\pi R^2(nh, i\tau) + \pi R^2(0, i\tau)}\right)^2 + 1960H}\Bigg)\Bigg] \\[3ex]
\dfrac{C((n+1)h, i\tau) - C(nh, i\tau)}{h} = \dfrac{\pi}{Q}(d + 2R(nh, i\tau))[2\alpha(C_s - \\
\quad C(nh, i\tau))\Bigg(\sqrt{\left(\dfrac{2Q}{\pi R^2(nh, i\tau) + \pi R^2(0, i\tau)}\right)^2 + 1960H}\Bigg)\Bigg]
\end{cases}
\quad (6)
$$

Setting $\frac{2M}{\rho_s}C_s\tau = a, \frac{2M}{\rho_s}\tau = b, \frac{2}{Q}C_s\pi h = A, \frac{2}{Q}\pi h = B$, we obtain the following:

$$
\begin{cases}
R_{i+1}^n = \alpha\Bigg(\sqrt{\left(\dfrac{2Q}{\pi(R_i^n)^2 + \pi(R_i^0)^2}\right)^2 + 1960H}\Bigg)(a - bC_i^n) + R_i^n \\[3ex]
C_i^{n+1} = \alpha\Bigg(\sqrt{\left(\dfrac{2Q}{\pi(R_i^n)^2 + \pi(R_i^0)^2}\right)^2 + 1960H}\Bigg)(A - BC_i^n)(d + 2R_i^n) + C_i^n
\end{cases}
\quad (7)
$$

Which leads to the following:

$$
\begin{cases}
R_i^0 = \alpha\Bigg(\sqrt{\left(\dfrac{2Q}{\pi(R_{i-1}^0)^2 + \pi(R_{i-1}^0)^2}\right)^2 + 1960H}\Bigg)(a - bC_{i-1}^0) + R_{i-1}^0 \\[3ex]
C_0^n = \alpha\Bigg(\sqrt{\left(\dfrac{2Q}{\pi(R_0^{n-1})^2 + \pi(R_0^0)^2}\right)^2 + 1960H}\Bigg)(A - BC_0^{n-1})(d + 2R_0^{n-1}) + C_0^{n-1}
\end{cases}
\quad (8)
$$

Using the initial conditions $R(x,0) = 0$ and $C(0,t) = C_0$, and the recursion formula (Eq. (8)), R_0^n, C_i^0 can be obtained; thus, all the initial conditions are obtained.

With the known initial condition R_0^n and R_i^n obtained from explicit difference formula, $\begin{cases} C_i^n \\ R_i^n \end{cases}$ can be derived by the chasing method and $\begin{cases} C_i^{n-1} \\ R_i^{n-1} \end{cases}$, and the numerical solution to Eq. (4) is archived.

The test parameters were as follows: $M = 58.5$ g/mol, $C_0 = 0$ mol/cm^3, $C_s = 0.0054$ mol/cm^3, $d = 0.6$ cm, ρ_s, Q, and $D/$

Table 5 Parameters for rock salt dissolution model from inversion results

Q L/h	Transformation coefficient α	Fitness value f	Relevant coefficient
10	0.00001689	0.01661	0.9977
20	0.00002404	0.04521	0.9959
30	0.00003287	0.04794	0.9951
40	0.00003823	0.06467	0.9966

δ were empirically derived and are shown in Tables 2, 3, and 4. Thus, the parameters $a, b, A,$ and B could be calculated to acquire.

Parameters inversion

The formula of the dissolved radius and weight of the rock salt weight was established in Ren et al. (2011):

$$R(k) = \sqrt{\frac{m(k)}{\rho_s l \pi} + \frac{d^2}{4}} - \frac{d}{2} \qquad (9)$$

where $R(k)$ is the dissolved radius of rock salt for the kth test record, l is the height of the specimen, and $m(k)$ is the dissolved mass for test record k.

The fitness function can be established as follows:

$$f = \frac{1}{N} \sum_{k=1}^{N} \left(\sqrt{\frac{m(k)}{\rho_s l \pi} + \frac{d^2}{4}} - \frac{d}{2} - R \right) \qquad (10)$$

where N is the number of test records, for tests recorded every 3 min, the total test time in seconds is $t = N \times 180$.
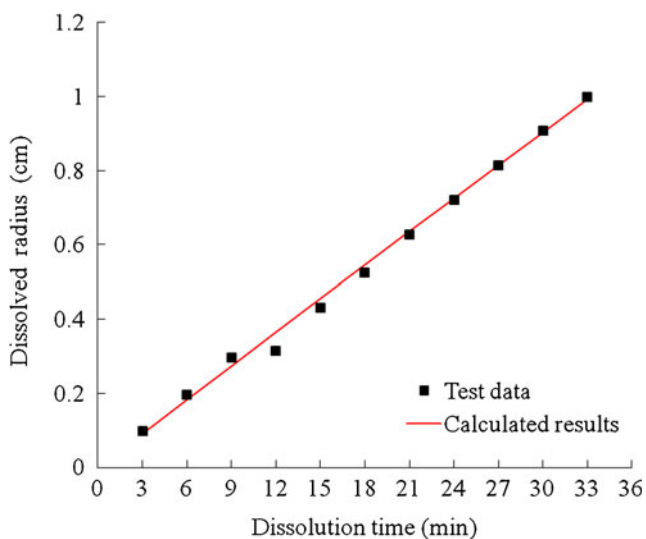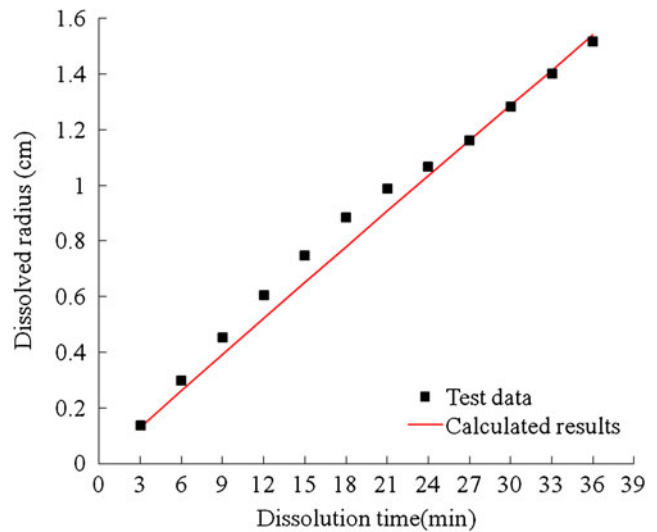
Fig. 9 Dynamic dissolved radius of rock salt with gravitational effect over time for flow rate of 20 L/h. Experimental results (*black squares*) and simulation results (*red line*)

Under gravitational effect, the dynamic dissolution model parameters of rock salt were obtained by parameters inversion (Table 5). A comparison of the experimental and simulation results for the dynamic dissolved radius of rock salt for flow rates of 10, 20, 30, and 40 L/h is shown in Figs. 8, 9, 10, and 11, respectively. The parameters inversion results show that the model and test results were in good agreement, indicating that under gravitational effect, the dynamic dissolution model of rock salt established in this paper provides a good estimate of the dynamic dissolution mechanism of rock salt. The results presented in this paper provide a theoretical basis and analytical means that can be used as a guide for studies on the dissolution mechanism of rock salt.
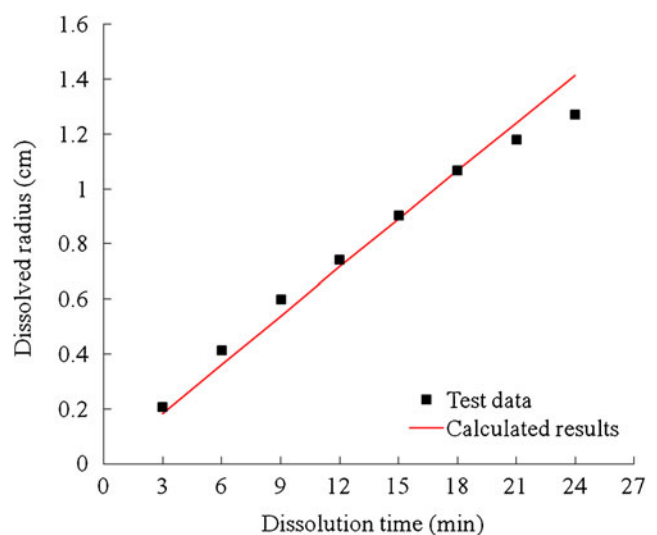
Fig. 8 Dynamic dissolved radius of rock salt with gravitational effect over time for flow rate of 10 L/h. Experimental results (*black squares*) and simulation results (*red line*)

Fig. 10 Dynamic dissolved radius of rock salt with gravitational effect over time for flow rate of 30 L/h. Experimental results (*black squares*) and simulation results (*red line*)
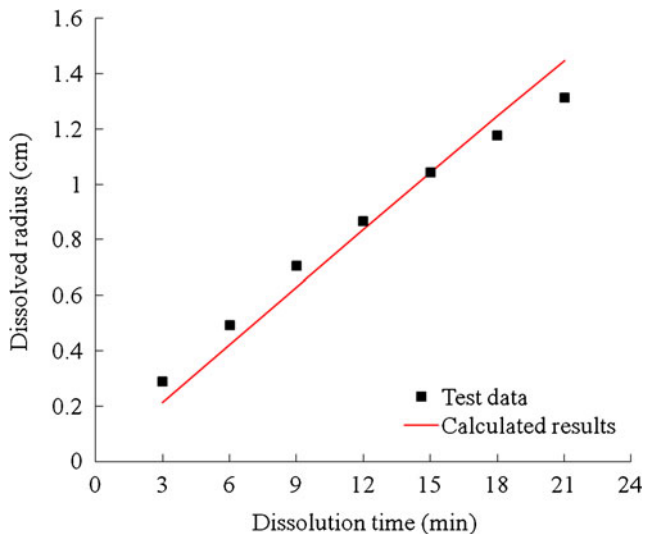
Fig. 11 Dynamic dissolved radius of rock salt with gravitational effect over time for flow rate of 40 L/h. Experimental results (*black squares*) and simulation results (*red line*)

Conclusions

Based on the dissolution characteristics of rock salt obtained in a laboratory experiment, the dynamic dissolution model under gravitational effect was established for different rates of water flow, dynamic dissolution characteristics were thoroughly and systematically examined, and the following conclusions were drawn:

(1) Using a custom-designed dynamic dissolution testing apparatus, the dynamic dissolution process of rock salt under the effect of gravity at different water flow rates was investigated. Under gravitational effect at flow rates of 20, 30, and 40 L/h, the average dissolution rates were 5.9733, 6.2838, and 7.9548 g/min, respectively, these dissolution rates were 2.1041, 1.6848, and 1.4635 times those calculated without considering the gravitational effect, indicating that gravity increased the flow velocity and accelerated the dissolution of rock salt.

(2) Based on the dissolution characteristics of rock salt obtained in the experiment, the effect of different parameters of the dissolution model was analyzed. The analysis indicated that the parameter D/δ was linearly related to the flow velocity and established the dynamic dissolution model under the effect of gravity.

(3) Using the finite difference method, a numerical solution of the dynamic dissolution model of rock salt was obtained. The simulation results based on parameter inversion were consistent with the experimental result, indicating that the dynamic dissolution model of rock salt established in this paper provides a reliable description of the dissolution mechanism of rock salt subjected to gravity.

References

Cosenza P, Ghoreychi M, Bazargan-Sabet B, de Marsily G (1999) In situ rock salt permeability measurement for long term safety assessment of storage. Int J Rock Meck Min Sci 36(4):509–526

Hampel A, Schulze O (2007) The composite dilatancy model: a constitutive model for the mechanical behavior of rock salt. In: Wallner M, Lux K-H, minkley W, Hardy H R Jr, (ed). The Mechanical Behavior of Salt-Understanding of THMC Process in Salt, Taylor & Francis Group, 99–107

Jessen FW (1972) Progress report-1)Rate of solution of salt under turbulent flow conditions, 2) study of mixing effects in salt water, 3) Mechanism of solution and cavity control using intermediate injection, 4) Investigation of multiple well system, Solution mining Research Institute file 72-0009-SMRI

Jiang DY, Chen J, Liu JP, Zhou LJ, Wang CR (2009) Experimental research on acoustic and dissolved properties of stress damaged salt rock. Rock Soil Mech 30(12):3569–3573 (In Chinese)

Liang WG, Zhao YS, Xu SG, Dusseault B (2008) Dissolution and seepage coupling effect on transport and mechanical properties of glauberite salt rock. Transp Porous Med 74(2):185–189

Liu CL, Xu LJ, Xian XF (2002) Fractal-like kinetic characteristics of rock salt dissolution in water. Colloid Surf A 201(1–3):231–235

Liu XR, Yang X, Zhong ZL, Liang NH, Wang JB, Huang M (2015) Research on dynamic dissolving model and experiment for rock salt under different flow conditions. Adv Mater Sci Eng. doi:10.1155/2015/959726

Ma HL, Chen F, Yang CH, Shi XL, Zhang M (2010) Experimental research on dissolution rate of salt rock in depth. Min Res Dev 30(5): 9–13 (In Chinese)

Ren S, Yang C, Jiang D, Li X, Song S (2011) Development of a new triaxial testing machine with high temperature for dissolution characteristics of salt rock and its application. Chin J Rock Mech Eng 30(2):289–295 (In Chinese)

Stormont JC (1997) In situ gas permeability measurements to delineate damage in rock salt. Int J Rock Meck Min Sci 34(7):1055–1064

Tang YC, Fang JN, Zhou H (2012) Study of rock salt dissolving characteristics test with triaxial stress effect. Rock Soil Mech 33(6):1601–1607 (In Chinese)

Tsang CF, Bemier F, Davies C (2005) Geohydromechanical processes in the excavation damaged zone in crystalline rock, rock salt, and indurated and plastic clays-in the context of radioactive waste disposal. Int J Rock Meck Min Sci 42(1):109–125

Wawersik WR (1981) Creep testing of salt: procedures, problem and suggestions. The First Conference on Mechanical Behaviors of Salt, Trans Tech Publication, 421–429

Yang CH, Jing WJ, Daemen JJK, Zhang GM, Du C (2013) Analysis of major risks associated with hydrocarbon storage caverns in bedded salt rock. Reliab Eng Syst Saf 113:94–111

Zhou H, Tang YC, Hu DW, Feng XT, Shao JF (2006) Study on coupled penetrating-dissolving model and experiment for salt rock cracks. Chin J Rock Mech Eng 25(5):946–950 (In Chinese)